

Supplemental Information For

Silicon Nanoparticles: Are they Crystalline from the Core to the Surface?

Alyxandra N. Thiessen[§] *Michelle Ha*,[§] *Riley W. Hooper*, *Haoyang Yu*, *Anton O. Oliynyk*,
Jonathan G. C. Veinot,* and *Vladimir K. Michaelis**

Department of Chemistry, University of Alberta, Edmonton, Alberta, Canada, T6G 2G2

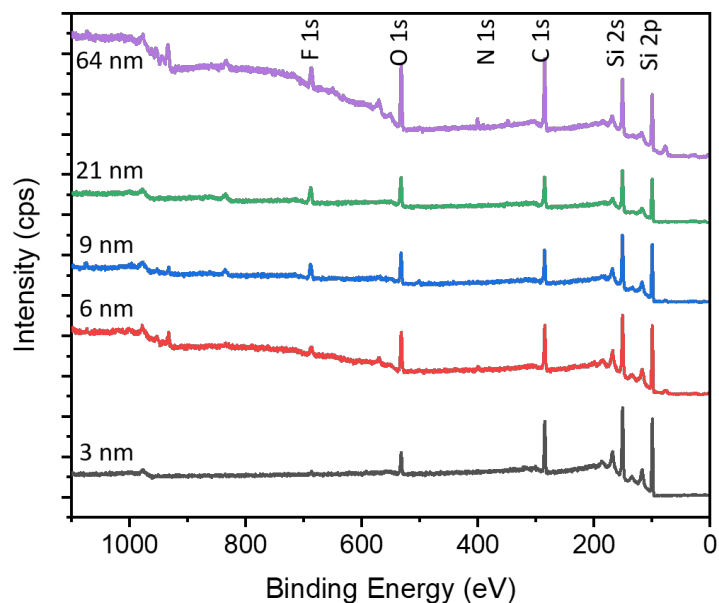
***Corresponding author:**

Jonathan G.C. Veinot: jveinot@ualberta.ca

Vladimir K. Michaelis: vladimir.michaelis@ualberta.ca

Table of Contents

Figure S1: Survey XPS data, tabulated elemental composition and peak composition	3
Figure S2: XPS peak fitting	4
Figure S3: Size distributions	5
Figure S4: XRD alignment with (a) LaB ₆ (NIST) and (b) Si standards.....	5
Figure S5: T_1 buildup curves for H-SiNPs	6
Figure S6: FTIR data for H-SiNPs	6
Figure S7: XRD peak broadening distribution for nanocrystalline materials.....	7
Figure S8: Contact time array for ²⁹ Si CPMAS NMR	7
Figure S9: NMR data for oxidized 9 nm H-SiNPs	8
Figure S10: XPS and FTIR data for 6 nm H-SiNPs after running NMR.....	8
Figure S11: Deconvolution of NMR data for surface/subsurface	9
Table S1: List of common chemical shifts for silicon-containing materials	9
Table S2: Estimated Si content in structural components.....	9
References	10

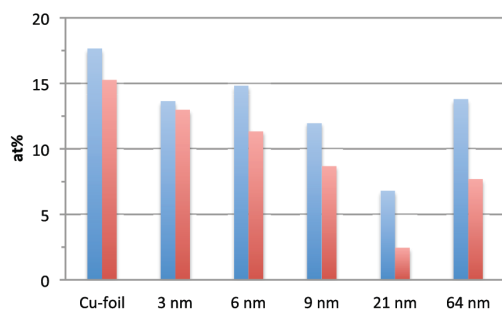


Elemental composition from survey

Sample	C at%	O at%	Si at%	F at%	Cu at%
Cu foil	72.08	17.65	0	0	5.79
3 nm	40.48	13.64	38.08	7.8	0
6 nm	36.66	14.81	44.27	4.25	0
9 nm	36.23	11.97	44.88	6.53	0.39
21 nm	42.07	6.79	50.25	0.88	0
64 nm	40.25	13.79	42.56	2.76	0.63

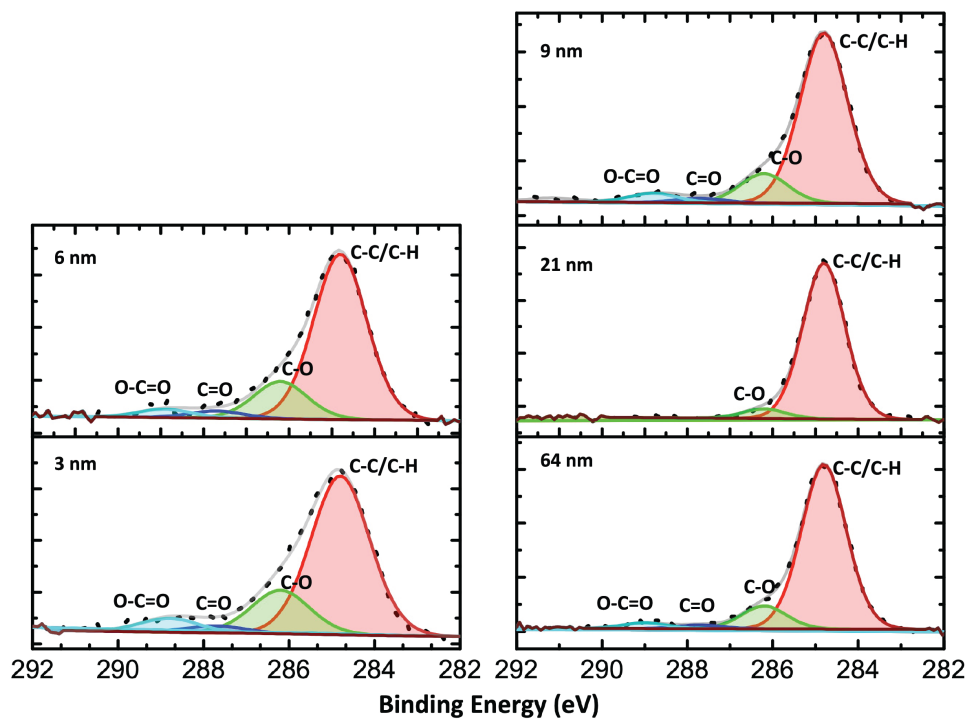
Peak composition from C 1s

C 1s	C 1s				Si 2p	
	C-C/C-H	C-O	C=O	O-C=O	eV	
Cu foil	87.37	8.74	3.35	4.54	3 nm	99.43
3 nm	74.01	17.88	2.01	6.1	6 nm	99.48
6 nm	74.07	17.1	3.88	4.95	9 nm	99.37 99.57 (10%)
9 nm	78.46	13.53	2.04	4.2	21 nm	99.42
21 nm	94.17	5.83	0	0	64 nm	99.43
64 nm	83.72	11.59	1.87	2.82		



	O at% from survey	O at% from C 1s
Cu-foil	17.65	15.26
3 nm	13.64	12.99
6 nm	14.81	11.32
9 nm	11.97	8.68
21 nm	6.79	2.45
64 nm	13.79	7.69

Figure S1: Survey XPS data for 3 nm (black), 6 nm (red), 9 nm (blue), 21 nm (green) and 64 nm (purple), tabulated elemental composition and peak composition for C and O atomic % (at%) from survey.



Red= crystalline core
Blue= surface Si atoms
Orange= disordered Si network
Green= Si oxides

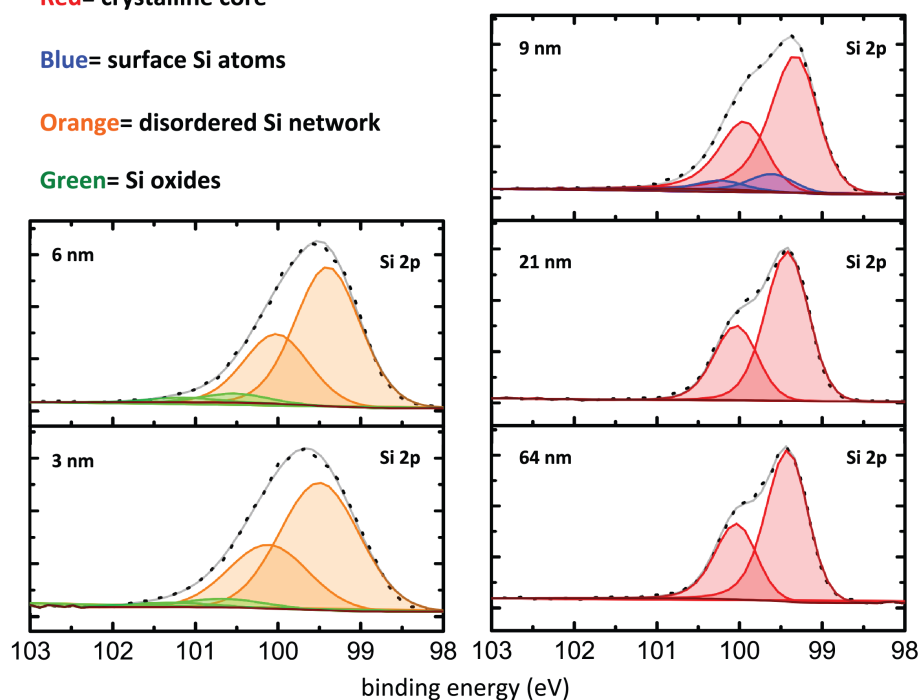


Figure S2: Peak fitting for C and Si XPS data for 3, 6, 9, 21, and 64 nm nanoparticles.

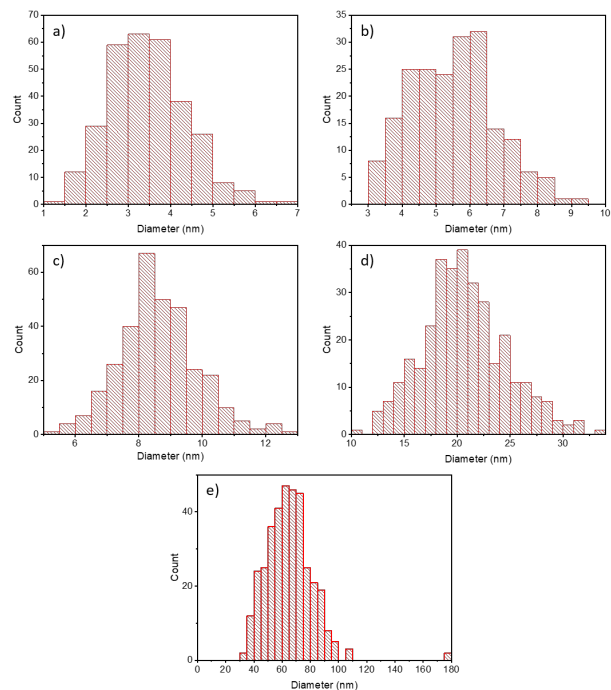


Figure S3: Histograms showing size distributions for (a) 3 nm, (b) 6 nm, (c) 9 nm, (d) 21 nm, and (e) 64 nm H-SiNPs.

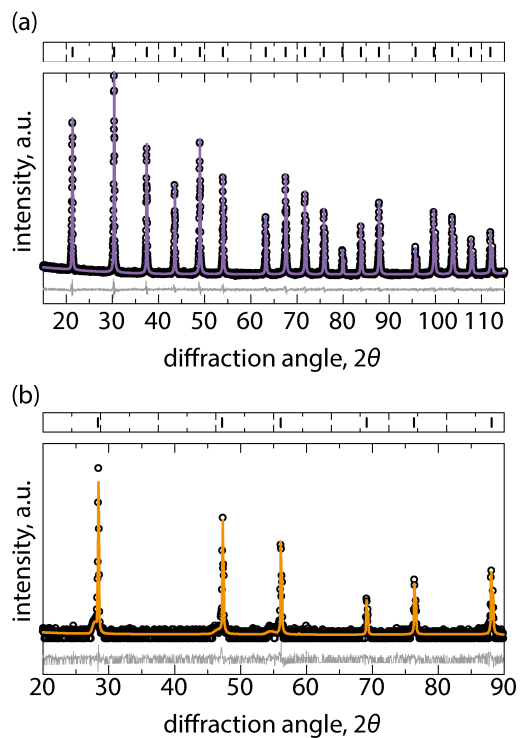


Figure S4. XRD alignment with (a) LaB₆ (NIST) and (b) Si standards.

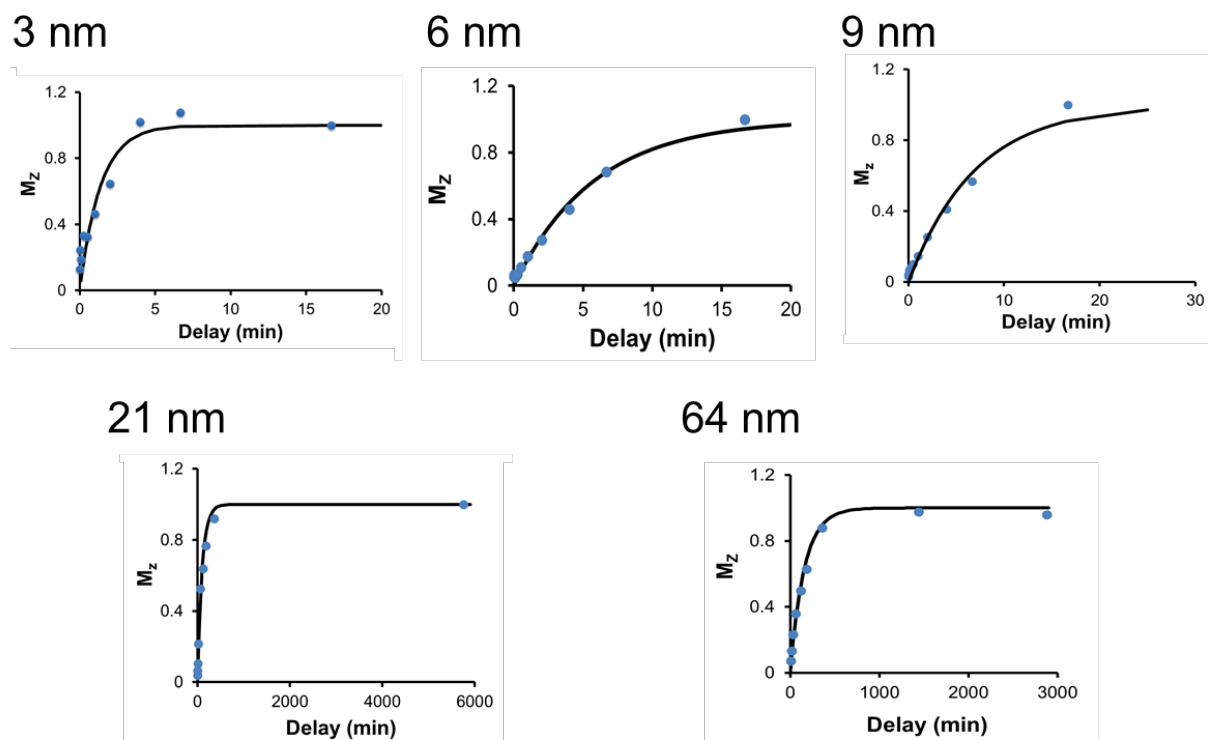


Figure S5: T_1 buildup curves for H-SiNPs, fitted using a mono-exponential longitudinal magnetization recovery for smaller H-SiNPs (3 and 6 nm) and a bi-exponential recovery for larger H-SiNPs (9, 21, and 64 nm).

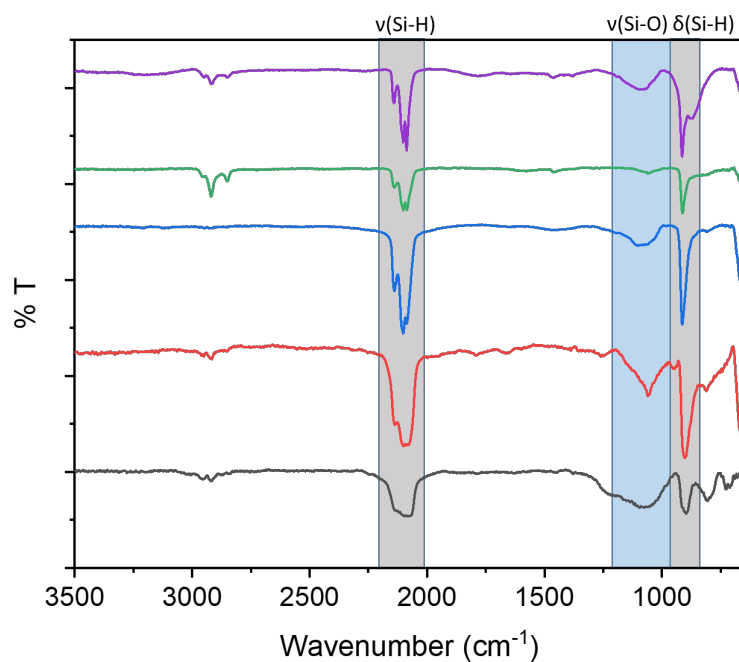


Figure S6: FTIR spectra for H-SiNPs annealed at 1500 °C (purple), 1400 °C (green), 1300 °C (blue), 1200 °C (red), and 1100 °C (black). The spectra show peaks associated with Si-H (highlighted in gray) and Si-O (highlighted in blue).

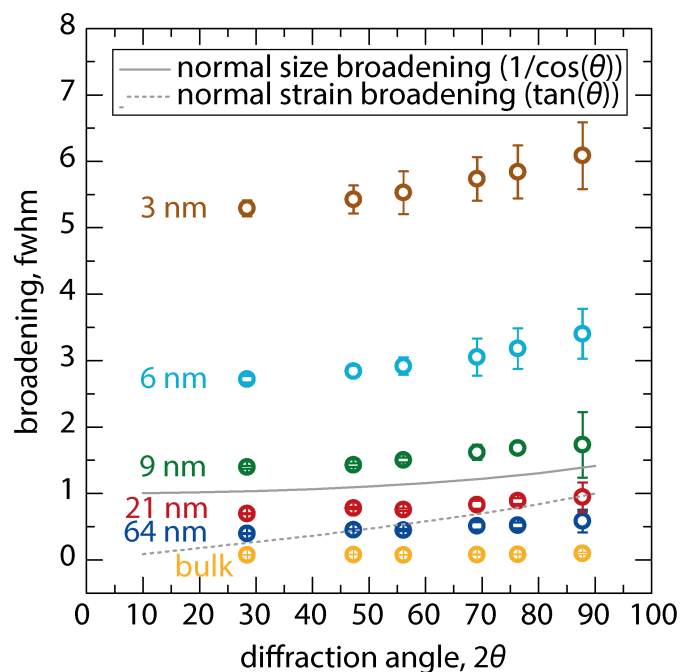


Figure S7. XRD Peak broadening distribution for nanocrystalline materials.

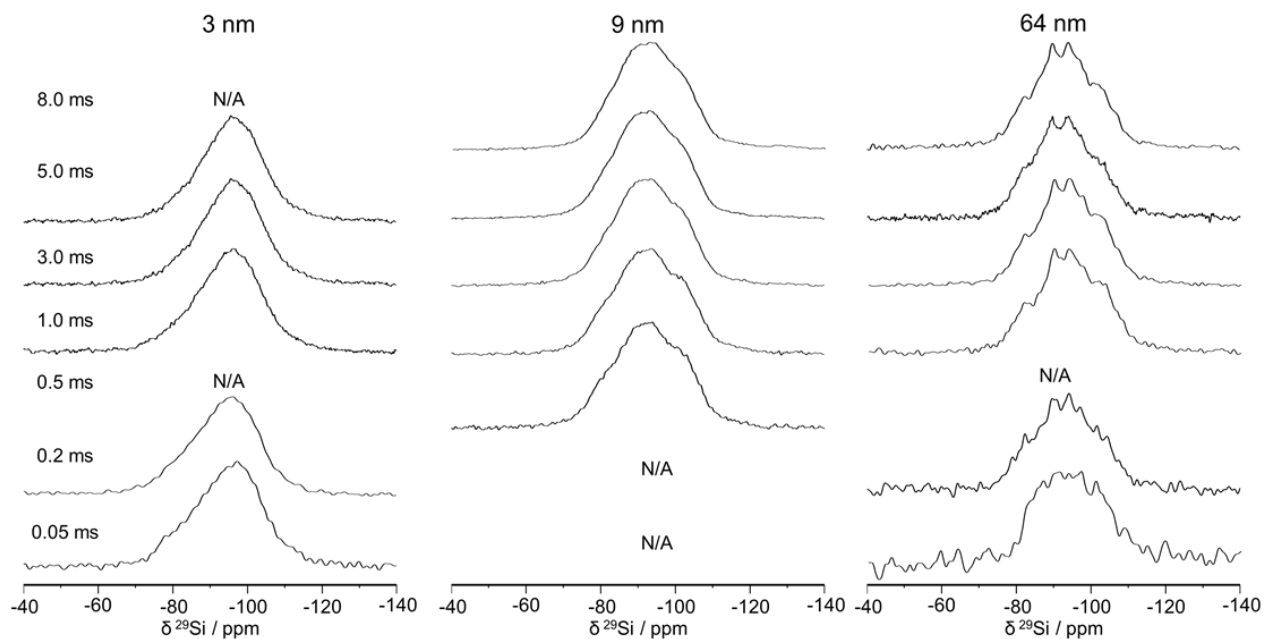


Figure S8: Contact time array for ^{29}Si CP MAS ranging from 0.05 to 8.0 ms for 3, 9, and 64 nm H-SiNPs.

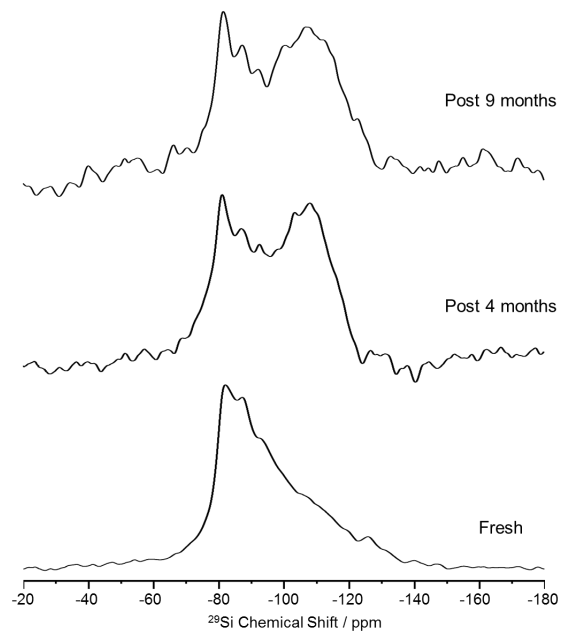


Figure S9: Silicon-29 NMR spectra for 9 nm H-SiNPs purposefully oxidized over a period of 9 months to illustrate the effect on the NMR spectra of contamination by oxygen under ambient storage. Presence of Si-O species at δ_{iso} of ~ -110 ppm 4 and 9 months post-synthesis.

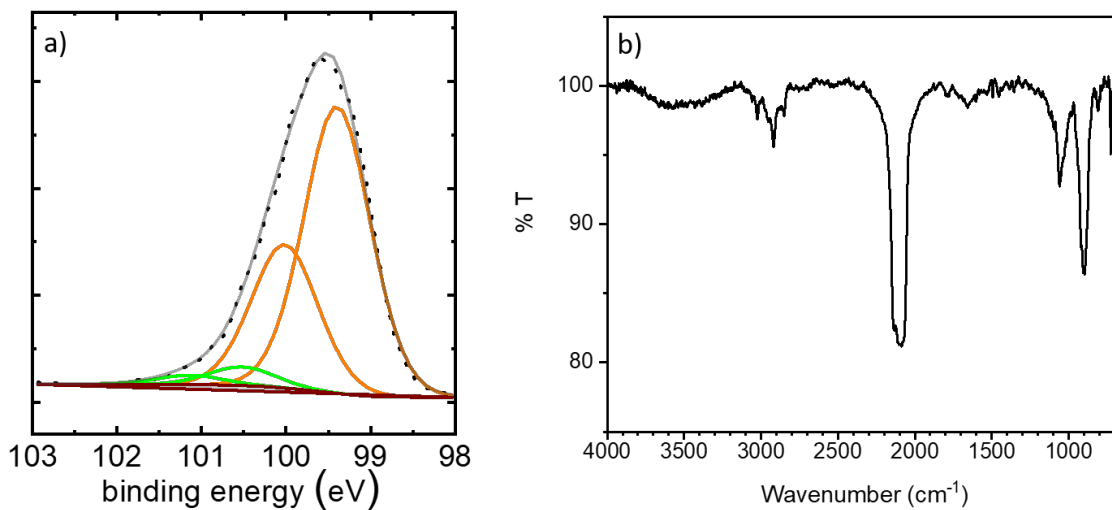


Figure S10: Sample of the post-NMR analysis of the H-SiNPs (6 nm) using (a) Si 2p high resolution XPS data (with only the $2p_{3/2}$ shown for clarity) and (b) FTIR spectra of 6 nm H-SiNPs.

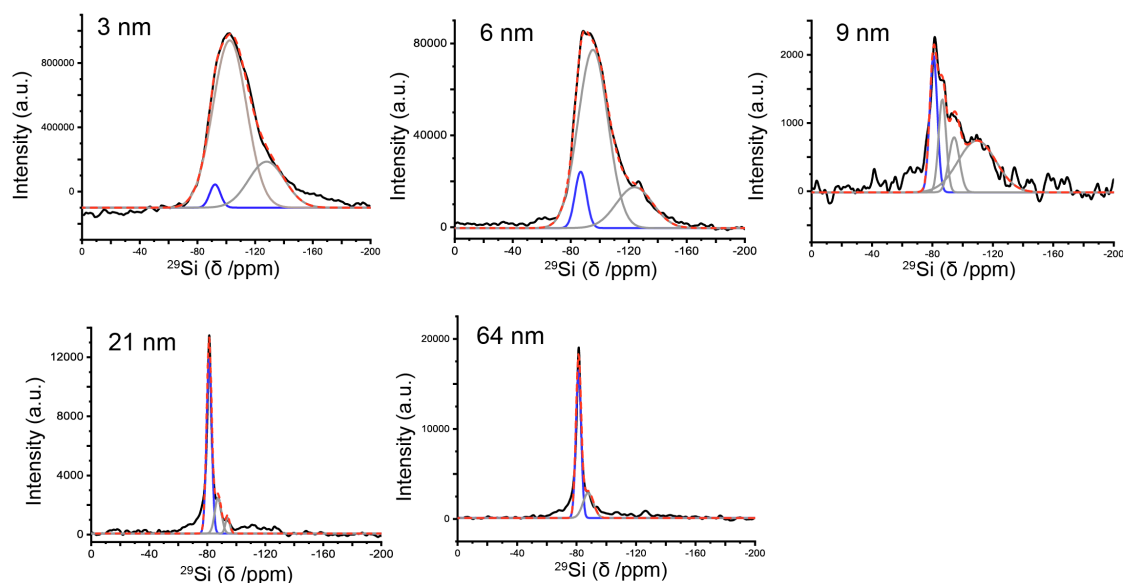


Figure S11: Estimated core (blue) vs surface/subsurface (grey) fractions from ^{29}Si MAS NMR (Bloch) using appropriate delay times (i.e., $5 \times T_1$). The black line is the experimental data and the red dashed line is the fitting envelope.

Table S1: List of common ^{29}Si chemical shifts for silicon containing materials.

Bonding Environment	Chemical Shift (ppm)	Ref
Amorphous – SiO_2	-110	
Quartz – SiO_2	-107	4, 5
Cristobalite – SiO_2	-109	
SiO_5 / SiO_6	-150 / -200	4
SiN_4	-49 (^{14}Si) / -225 (^{6}Si)	4, 6
SiC_4	-18	4
OSi-H_x / $\text{HO-Si(-OSiH}_x)_x$	-89 to -109	7, 8, 9
$-\text{SiH}_3$ / $-\text{SiH}_2$ / $-\text{SiH}$	-90 to -110	10,11
Molecular – $\text{H}_3\text{Si-SiH}_3$; $\text{H}_2\text{Si(-SiH}_3)_2$; $\text{HSi(-SiH}_3)_3$; $\text{Si(-SiH}_3)_4$	-103 to -165	9, 12

Table S2: Calculated fraction of surface, sub-surface and core Si species based on the model by Zhao *et al.* and Avramov *et al.*^{2,3}

Particle Size /nm	Estimated % Fraction of atoms in each structural component		
	Surface	Subsurface	Core
64	1	4	95
21	5	17	78
9	11	37	52
6	17	50	33
3	27	62	11

REFERENCES

1. Comedi, D.; Zalloum, O. H. Y.; Irving, E. A.; Wojcik, J.; Roschuk, T.; Flynn, M. J.; Mascher, P. X-Ray Diffraction Study of Crystalline Si Nanocluster Formation in Annealed Silicon-Rich Silicon Oxides. *J. Appl. Phys.* **2006**, *99*, 023518.
2. Zhao, Y.; Kim, Y.-H.; Du, M.-H.; Zhang, S. B. First-Principles Prediction of Icosahedral Quantum Dots for Tetravalent Semiconductors. *Phys. Rev. Lett.* **2004**, *93*, 015502.
3. Avramov, P. V. F., D. G.; Sorokin, P. B.; Chernozatonskii, L. A.; Gordon, M. S. New symmetric families of silicon quantum dots and their conglomerates as a tunable source of photoluminescence in nanodevices. *Los Alamos Natl. Lab, Prepr. Arch., Condens. Matter* **2007**, p. 1. <https://arxiv.org/abs/0709.2279> (accessed July 17, 2018).
4. MacKenzie, K.J.D.; Smith, M.E. Multinuclear Solid-State NMR of Inorganic Materials; Pergamon Materials Series; Elsevier Science: Oxford, UK, 2002; Chapter 4, pp. 201-268.
5. Smith, J. V.; Blackwell, C. S. Nuclear Magnetic Resonance of Silica Polymorphs. *Nature*, **1983**, *303*, 223.
6. Sekine, T.; Tansho, M.; Kanzaki, M. Si-29 Magic-Angle-Spinning Nuclear-Magnetic-Resonance Study of Spinel-Type Si₃N₄. *Appl. Phys. Lett.* **2001**, *78*, 3050–3051.
7. Neiner, D.; Kauzlarich, S.M. Hydrogen-Capped Silicon Nanoparticles as a Potential Hydrogen Storage Material: Synthesis, Characterization, and Hydrogen Release. *Chem. Mater.* **2010**, *22*, 487-493.
8. Lee, D.; Kaushik, M.; Coustel, R.; Chenavier, Y.; Chanal, M.; Bardet, M.; Dubois, L.; Okuno, H.; Rochat, N.; Duclairoir, F.; Mouesca, J-M.; De Paëpe, G. Solid-State NMR and DFT Combined for the Surface Study of Functionalized Silicon Nanoparticles. *Chem. Eur. J.* **2015**, *21*, 16047-16058.
9. Faulkner, R. A.; DiVerdi, J. A.; Yang, Y.; Kobayashi, T.; Maciel, G. E. The Surface of Nanoparticle Silicon as Studied by Solid-State NMR. *Materials* **2013**, *6*, 18–46.
10. He, J.; Ba, Y.; Ratcliffe, C. I.; Ripmeester, J. A.; Klug, D. D.; Tse, J. S.; Preston, K. F. Encapsulation of Silicon Nanoclusters in Zeolite Y. *J. Am. Chem. Soc.* **1998**, *120*, 10697–10705.
11. Petit, D.; Chazalviel, J.N.; Ozanam, F.; Devreux, F. Porous Silicon Structure Studied by Nuclear Magnetic Resonance. *Appl. Phys. Lett.* **1997**, *70*, 191–193.
12. Hahn, J. Breitrage zur Chemie des Siliciums und Germaniums, XXIX ²⁹Si-NMR-Spektroskopische Untersuchungen von Geradkettigen und Verzweigten Silanen. *Z. Naturforsch.* **1980**, *35*, 282–296.